

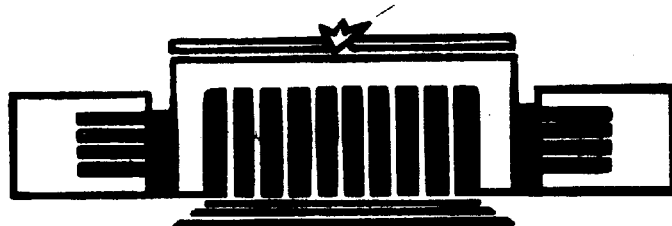


ИНСТИТУТ ЯДЕРНОЙ ФИЗИКИ СО АН СССР

**Boris V. Chirikov**

**INTRINSIC STOCHASTICITY**

**PREPRINT 84-147**



НОВОСИБИРСК

Institute of Nuclear Physics

Boris V.Chirikov

INTRINSIC STOCHASTICITY

Preprint

Novosibirsk

# INTRINSIC STOCHASTICITY

Boris V. Chirikov

Institute of Nuclear Physics,  
630090 Novosibirsk, U.S.S.R.

## A b s t r a c t

Selected topics in the theory of dynamical chaos in Hamiltonian systems are discussed, including the nature and mechanism of the chaos as well as its peculiar statistical properties in presence of the chaos border with a critical scale-invariant structure. As an example, two simple models described by two-dimensional mappings are considered.

## 1. Introduction

The dynamical chaos, or intrinsic stochasticity, means the random (irregular) motion of a completely deterministic (dynamical) system which is free of any noise, either external or internal. The discovery and explanation of those controversial processes has been one of the most fundamental recent achievements in the classical mechanics. The dynamical chaos should not be confused with the motions described by the so-called stochastic equations which represent just the effect of noise upon a dynamical system. Sometimes dynamical chaos may be useful, e.g., for particle heating by an electromagnetic wave in plasma (see, e.g., /1/ for review). However, in most cases it is harmful as it means a global instability of motion, e.g., the collisionless leakage of particles out of a magnetic trap /2/.

The account of dynamical chaos is most important in simple systems with just a few degrees of freedom. For example, a single particle in magnetic trap has only three degrees of freedom or even two, in an axisymmetric magnetic field. Another important example is the geometry of magnetic field itself whose lines can be considered as trajectories of certain dynamical system. For all those systems one cannot simply introduce some statistical assumptions, e.g., ergodicity, as is usually done in the statistical mechanics. Instead, it is necessary to study the dynamics of a particular system, and to find out if its motion is regular or chaotic. This depends on the system parameters as well as on the initial conditions of its motion. In a conventional mirror trap, for example, a domain of chaotic motion does always exist near the adiabatic loss cone, expanding the latter (Fig. 1). For a harmonic magnetic shape, and for a sufficiently small particle velocity  $v$  the chaos border is given by the relation /2/

$$\Delta\beta_0 \approx 4.2 \frac{r_0}{L} (\lambda q)^2 e^{-q}; \quad q = \frac{4}{3\pi\sqrt{\lambda-1}} \cdot \frac{L\omega_c}{v} \quad (1.1)$$

Here  $\Delta\beta_0$  is the pitch-angle width of the chaotic layer,  $r_0$  the gyrocenter radius,  $\omega_c$  the gyrofrequency (all in the

midplane),  $\lambda$  the mirror ratio, and  $2L$  is the distance between mirrors.

Generally, the statistical properties of chaotic motion are not as simple as in standard statistical hypotheses or in stochastic equations, e.g., the usually assumed exponential correlation decay. The complexity of dynamical chaos is related, particularly, to the chaos border in phase space whose vicinity has an intricate hierarchical structure including domains of both chaotic as well as regular motions. In the above example of a magnetic mirror trap it results, particularly, in a nonexponential relaxation (leakage) of particles. It is quite likely that just this effect had been observed in the experiments by Varma and coworkers which were reported at the Conference in Nagoya /3/, and also were discussed then in Rosenbluth's summary. An example of that relaxation (after Ref. /4/) is depicted in Fig. 2. The authors interpreted it in terms of the sum of exponentials with different characteristic times  $\tau_c$ . However, rescaled as a log-log plot, the data fit also fairly well a power law dependence. Below we are going to explain why the latter dependence is to be expected (Sect. 6).

## 2. The Nature of Dynamical Chaos

Since the time of Poincaré it appeared intuitively clear that irregular dynamical motion is explained by its strong (exponential) local instability. However, the progress in the modern ergodic theory has led to a paradoxical conclusion that such an instability by itself does not imply almost any statistical properties of the motion. Particularly, the correlation not only decays nonexponentially, in general, but may even not decay to zero at all if the motion spectrum possesses a discrete component. Of course, the exponential instability of chaotic motion does imply some continuous component in the spectrum unlike regular (quasiperiodic) motion whose spectrum is purely discrete.

The above controversy is resolved in the new, algorithmic theory of dynamical systems on the basis of the exactly formulated mathematically (and perfectly reasonable from the physical viewpoint) concept of random dynamical trajectory (see

/5,6/ and an elementary presentation in Ref. /7/). The principal point here is the algorithmic independence of any sufficiently long segments on such a trajectory. It means impossibility, in any way, to calculate (predict) a single segment from the observation even all the rest together. In other words, the information  $J(t)$  contained in a random trajectory (as recorded to any finite accuracy  $\varepsilon$ , of course) grows in proportion to its length:

$$\lim_{t \rightarrow \pm \infty} \frac{J(t)}{|t|} = h > 0 \quad (2.1)$$

where the KS-entropy

$$h = \sum \Lambda_+ \geq \Lambda_{\max} \quad (2.2)$$

describes the mean rate of the local exponential instability, and  $\Lambda_{\max} \geq \Lambda_+ > 0$ . Note that mean information flow (2.1) does not depend on the accuracy  $\varepsilon$ . Indeed, decrease in  $\varepsilon$  implies an increase of the algorithmic correlation time  $\tau_a \sim h^{-1} |\ln \varepsilon|$ . Hence,  $J(t)/|t| \sim |\ln \varepsilon| / \tau_a \sim h$ .

An important corollary of these simple considerations is the existence of a continuous transition between deterministic and random behavior of a chaotic trajectory. The transition is described by the randomness parameter /8/:

$$Q(t) = \frac{h|t|}{|\ln \varepsilon|} \sim \frac{|t|}{\tau_a} \quad (2.3)$$

A temporary, or transient, determinism ( $Q \ll 1$ ;  $|t| \ll \tau_a$ ) gets over eventually to the asymptotic randomness ( $Q \gg 1$ ,  $|t| \gg \tau_a$ ).

On the other hand, the quasiperiodic (regular) motion is characterized by a linear in time (weak) instability (see, e.g., Ref. /10,9/). Hence, for a regular trajectory  $J(t) \sim \ln |t|$ . Since  $J(t)/|t| \rightarrow 0$  as  $t \rightarrow \pm \infty$ , the prediction of any trajectory segment is possible from the observation of a neighboring segment with a comparable length<sup>\*)</sup>.

\*) The opposite conclusion due to Born /10/ on unpredictability of a quasiperiodic trajectory is related to the fact that he considered prediction from the initial conditions only, and not from a finite trajectory segment.

An interesting and instructive example of the interplay between deterministic and random features of dynamical chaos is the electron motion in a "braided" toroidal magnetic field with random lines /11/. Configuration of such a field is characterized by the radial diffusion of magnetic lines:

$\langle (\Delta r)^2 \rangle \propto \ell$  where  $\ell$  is the line length. If one would completely neglect both the electron scattering and all the finite gyroradius effects the electron diffusion were the same with  $\ell = |v_{||} t|$ . However, if only the scattering is taken into account but not the drift, nor a shift of guiding center, then, by virtue of motion reversibility along a magnetic line (even a chaotic one!) subsequent to a change of  $v_{||}$  sign,  $\langle \ell^2 \rangle \propto t$ , and  $\langle (\Delta r)^2 \rangle \propto \sqrt{t}$  /11/. Also, generally, the chaotic motion is reversible, and its statistical relaxation proceeds for both directions in time as  $t \rightarrow \pm \infty$  /12/.

All the complexity of a random trajectory, i.e. all its past and future chaos, is completely contained in the exactly fixed (imaginarily!) initial conditions. It means that the ultimate origin of dynamical chaos relates to the continuity of phase space in classical (but not quantum!) mechanics. The proper dynamical system is only to provide the exponential instability ( $h > 0$ ), and therefore it may be very simple that still appears so paradoxical.

### 3. Statistical Properties of Hamiltonian Dynamics

For a trajectory of dynamical system to be random it is necessary and sufficient, according to the Alekseev-Brudno theorem /5,6/, that  $h > 0$ , or equivalently, that the maximal Lyapunov exponent  $\Lambda_{\max} > 0$ . This is apparently the simplest numerical test for randomness. However, the randomness by itself implies only that the very concept of trajectory loses its direct physical meaning like that of unstable equilibrium or of unstable periodic orbit. The dynamical chaos has to be described in terms of statistical mechanics, yet its statistical properties may be very different. They are determined, to a large extent, by the behavior of correlations or, correspondingly, by the type of motion spectrum. A simple ("routine") statistic relates to the exponential correlation decay and to

An interesting and instructive example of the interplay between deterministic and random features of dynamical chaos is the electron motion in a "braided" toroidal magnetic field with random lines /11/. Configuration of such a field is characterized by the radial diffusion of magnetic lines:

$\langle (\Delta r)^2 \rangle \propto \ell$  where  $\ell$  is the line length. If one would completely neglect both the electron scattering and all the finite gyroradius effects the electron diffusion were the same with  $\ell = |v_{||} t|$ . However, if only the scattering is taken into account but not the drift, nor a shift of guiding center, then, by virtue of motion reversibility along a magnetic line (even a chaotic one!) subsequent to a change of  $v_{||}$  sign,  $\langle \ell^2 \rangle \propto t$ , and  $\langle (\Delta r)^2 \rangle \propto \sqrt{t}$  /11/. Also, generally, the chaotic motion is reversible, and its statistical relaxation proceeds for both directions in time as  $t \rightarrow \pm \infty$  /12/.

All the complexity of a random trajectory, i.e. all its past and future chaos, is completely contained in the exactly fixed (imaginarily!) initial conditions. It means that the ultimate origin of dynamical chaos relates to the continuity of phase space in classical (but not quantum!) mechanics. The proper dynamical system is only to provide the exponential instability ( $h > 0$ ), and therefore it may be very simple that still appears so paradoxical.

### 3. Statistical Properties of Hamiltonian Dynamics

For a trajectory of dynamical system to be random it is necessary and sufficient, according to the Alekseev-Brudno theorem /5,6/, that  $h > 0$ , or equivalently, that the maximal Lyapunov exponent  $\Lambda_{\max} > 0$ . This is apparently the simplest numerical test for randomness. However, the randomness by itself implies only that the very concept of trajectory loses its direct physical meaning like that of unstable equilibrium or of unstable periodic orbit. The dynamical chaos has to be described in terms of statistical mechanics, yet its statistical properties may be very different. They are determined, to a large extent, by the behavior of correlations or, correspondingly, by the type of motion spectrum. A simple ("routine") statistic relates to the exponential correlation decay and to



nonsingular spectrum at  $\omega = 0$ . In this case a simple statistical description by means of a kinetic (particularly, diffusion) equation is applicable. A complicated ("abnormal") statistic corresponds, in particular, to a power law dependence of correlations as  $t \rightarrow \pm \infty$ , and of spectral density as  $\omega \rightarrow 0$ . A well known example of such a behavior is the  $1/\omega$  noise.

As an example we shall consider a "simple" model /13/ described by the so-called standard mapping  $(\gamma, \theta) \rightarrow (\bar{\gamma}, \bar{\theta})$  where

$$\bar{\gamma} = \gamma + K \cdot \sin \theta; \quad \bar{\theta} = \theta + \bar{\gamma} \quad (3.1)$$

Here  $\gamma, \theta$  are action-phase variables, and  $K$  is the only parameter of the model. Many particular problems in nonlinear dynamics can be approximately reduced to this map, e.g., the particle motion in a mirror magnetic trap /2/ (for other examples, particularly, related to plasma physics, see Ref. /1/).

For  $K \gg 1$  the motion in  $\bar{\gamma}$  is described by a simple diffusion equation /13/, the diffusion rate being a complicated function of  $K$  though /14/. However, for special values of  $K \approx 2\pi n$ , where integer  $n \neq 0$ , the motion statistical properties become much more intricate /15-17/. In particular, the diffusion rate, formally determined numerically, grows indefinitely as the motion time increases. The origin of such statistical "anomalies"\*) relates to the chaos borders surrounding the domains of regular motion which occur for those special  $K$ . Notice that the chaos border is not the only origin of a complicated statistic. Apparently the most simple and graphic example of the latter is the so-called "stadium" model /18/.

In case of a regular motion the statistical description seems, at the first glance, to be completely inadequate. However, the question proves to be more "tricky". To see this consider for a moment the quantum dynamics, i.e. the evolution of a state vector  $\psi(t)$ . Here the motion (energy) spectrum is purely discrete for any conservative system bounded in the phase

---

\*) The quotes here intend to emphasize that those properties are anomalous to us, due to our previous experience in studying random processes, rather than to the Nature.

space. Hence, it appears to be no room for the dynamical chaos in quantum mechanics. Yet, the correspondence principle requires some transition to the classical motion, including a chaotic one as well. The resolution of this apparent contradiction has been given in Ref. /19/. The main idea is in imitation of some statistical properties of the classical chaos on a finite time scale of the quantum motion. In other words, in quantum dynamics a temporary, or transient, chaos is possible in spite of discrete spectrum. But the same is true for a regular classical motion as well! In this respect, I would like to attract reader's attention to a series of interesting papers due to Ott and coworkers /20/ dealing with some problems in plasma physics. However, it should be mentioned that no limitations of the classical chaos due to spectrum discreteness are taken into account in these papers.

#### 4. Resonant Theory of Critical Phenomena

The so-called critical phenomena occur, particularly, at the chaos border in phase space. First, we consider a simpler problem about a critical KAM (invariant) curve, e.g., one in the standard map (3.1). A KAM curve is specified by the mean frequency  $\langle \omega \rangle$  of phase rotation, or by the rotation number (frequency ratio)  $\nu = \langle \omega \rangle / 2\pi$ . For  $K = 0$  the curve  $y(\theta) = 2\pi\nu$  is just a straight line on the phase plane. If  $K \neq 0$  the curve is distorted:  $y(\theta) = y_r(\theta, K, \nu)$ . It becomes critical at certain  $K = K_c(\nu)$  when it is destroyed and bifurcates into some disjointed Cantor set, or a cantorus after Percival (see Ref. /21/), embedded into a narrow chaotic layer. The study of critical KAM curves had been started by Greene /22/, and was continued by many other authors, especially thoroughly by MacKay /23/. Here, the resonant theory of critical phenomena /24/ based upon the analysis of resonance structure near a critical KAM curve is briefly presented. One advantage of this approach is the possibility of approximate analytical calculation of many scale factors whose exact values are obtained only numerically. The resonant theory provides also some physical insight into the critical structure and, particularly,

leads to various relations between its parameters /24/\*). The results presented below have been obtained in collaboration with D.L. Shepelyansky /17,26/.

The structure of a critical KAM curve is intimately related to the arithmetical properties of its rotation number in the continued fraction representation

$$\nu = \frac{1}{m_1 + \frac{1}{m_2 + \frac{1}{m_3 + \dots}}} \equiv (m_1, m_2, m_3, \dots) \quad (4.1)$$

The convergents of this expansion

$$\nu_n = \frac{p_n}{q_n} = (m_1, \dots, m_n) \quad (4.2)$$

provide the best rational approximation to  $\nu$  with denominator  $q \leq q_n$ . From dynamical viewpoint the periodic trajectories with rotation numbers  $\nu_n$  correspond to the principal (strongest) resonances in a vicinity of curve  $\nu$ . They are outlined in Fig. 3 where the critical curve with  $\nu = \nu_c$  is chosen as the axis of the mean phase  $\langle \theta \rangle$  ( $\langle \dot{\theta} \rangle = 2\pi \nu_c$ ). For each resonance one period of its separatrix is shown (there are  $q_n$  such periods over the periodic trajectory, i.e. within the phase interval  $\langle \theta \rangle = 0 \div 2\pi$ ). Actually, each separatrix is embedded in a narrow chaotic layer, so that the whole critical structure is a capricious mosaic of both regular and chaotic motion components with a comparable measure.

The principal resonances determine the structure for corresponding scales of ever diminishing size which converge to the critical curve. The simplest critical structure relates to the so-called "golden" curve of  $\nu = \nu_g = (1, 1, \dots) = (\sqrt{5}-1)/2 \approx 0.618$  (see Refs. /22,23,27/\*). Asymptotically, as  $n \rightarrow \infty$  ( $q_n \rightarrow \infty$ ) all the scales here are exactly similar since the scaling factors are related to the ratio

\*) Still another approach to the study of critical KAM curves has been proposed earlier and is developing by Escande and co-workers /25/. Essentially, this theory is also a resonant one making use of the two-resonance approximation.

\*\*) This, exceptional in other respects, curve is believed to be the strongest one against perturbation, i.e. it gets destroyed at the biggest K /22/.

$S_n = q_n / q_{n-1}$  of denominators for successive convergents which rapidly approaches the limiting value  $S_g = 1/r_g = 1 + \sqrt{g} \approx 1.618$ .

The complete relationship of the structures at different scales is given by the so-called renormalization transformations which form a group. Such a renormgroup may be considered as an abstract dynamical system in the functional space of various mappings where the standard map, for example, is just a point. The serial scale number  $n$  is then a substitute for the time. This renormtime is thus proportional to the logarithm of characteristic size  $q_n^{-2}$  or of physical time  $q_n$  for a given scale  $n$  (see Ref. /24/).

In the problem under consideration the renormgroup, as well as the sequence of principal resonances, is discrete so that the corresponding abstract dynamical system is always a mapping (of the phase plane structure on two different scales). We shall call it renormmap for brevity. The asymptotic similarity on all the scales, or scale invariance, is the simplest dynamics of the renormmap, namely, a fixed point of saddle type.

A convenient and graphical way of presentation for a critical structure is the Fourier spectrum of motion on the critical curve or in its immediate vicinity. For a periodic trajectory, the Fourier amplitudes  $a_k$  are defined as follows:

$$\theta(t) = 2\pi r_N t + \sum_{k=1}^{[q_N/2]} a_k \cdot \sin(2\pi |\nu_k| t) \quad (4.3)$$

where  $t$  is discrete time (number of map iterations);  $q_N$  the motion period;  $r_N = p_N / q_N$  the rotation number, and  $|\nu_k| = k / q_N \leq 1/2$  the moduli of motion frequencies. By virtue of the time discreteness and of  $\theta(t)$  antisymmetry the amplitudes satisfy the relation  $a_{-\nu} = -a_\nu$ .

The largest amplitudes correspond to principal resonances, and, hence, to the motion frequencies, or detunes from exact resonance ( $\nu = 0$ )

$$\nu_n = q_n r_N - p_n \quad (4.4)$$

They are approximately described by the following empirical expression

$$\frac{A_n}{A_\infty} = \exp \left\{ C q_n [K_\ell(K, r_n) - K_G] \right\} = F(K, r_n) \quad (4.5)$$

Here we have defined the reduced amplitudes

$$A_n = q_n |a_n| \cdot |\sqrt{5} q_n \tilde{v}_n|^\mu \quad (4.6)$$

and some effective local perturbation

$$K_\ell(K, r_n) \approx K + K'_\ell (r_n - r_g) \quad (4.7)$$

which is fairly well approximated, according to our numerical data, by the linear dependence with "gradient"  $K'_\ell \approx 0.211$ . Note that Eq. (4.7) holds for the set of convergents  $r_n \rightarrow r_g$  only as function  $K_\ell(r)$  is apparently everywhere singular (fractal) according to Ref. /28/. We make use of a modified frequency

$$\tilde{\nu} = \frac{1}{\pi} \sin(\pi \nu) \quad (4.8)$$

which provides a better consistency of numerical data at large  $\nu$ . Eq. (4.5) is similar in structure to but different from one given by Escande (see Ref. /27/).

The empirical exponent  $\mu \approx 1.13$  in Eq. (4.6) takes account of the dependence on reduced detune  $\sqrt{5} q \tilde{\nu}$ , while numerical factor  $C \approx 1.2$  relates to deviations from the critical condition  $K_\ell = K_G$  where  $K_G = 0.97163540631...$  is Greene's critical  $K$  value for  $r = r_g$  /22,23,27/. Finally, the limiting amplitude, which characterizes the critical scale invariance, or the fixed point of renormmap, is equal numerically to

$$A_\infty = |q a|_\infty = 0.16736...; \quad |\sqrt{5} q \tilde{\nu}|_\infty = 1 \quad (4.9)$$

A convergence  $|q a|_n \rightarrow |q a|_\infty$  is shown in Fig. 4. The numerical data have been obtained from the periodic trajectory of  $q_N = 46368$  ( $|r_N - r_g| \approx 2 \times 10^{-10}$ ). Notice asymmetry between

two sides of the critical curve. In part, it is due to alternating detune  $|\sqrt{5}q\tilde{\nu}| - 1$ . Yet, for  $n \gtrsim 8$  the detune oscillation becomes negligible (it decays as  $q^{-2}$ ) but the asymmetry still persists because of the gradient term in Eq. (4.5) which decreases as  $q^{-1}$ .

Fourier amplitudes  $a_n$  of a critical curve are closely related to the phase plane structure of nearby resonances. Consider Fourier amplitudes of the perturbation  $v_n$  (in Hamiltonian) corresponding to frequencies  $\nu_n$  of the critical motion. As the latter is a driven oscillation it is reasonable to assume  $a_n \propto v_n / \tilde{\nu}_n^2$ . Using Eqs. (4.5) and (4.6) we arrive at

$$V_n = q_n^4 |v_n| \cdot |\sqrt{5}q\tilde{\nu}|_n^{\mu-2} = \varphi_\infty^2(r_g) \cdot F(K, r_n) \quad (4.10)$$

Here  $\varphi_\infty(r_g) = 1.047402 \dots$  is the limiting value of phase advance  $\varphi_n = q_n \Omega_n$  for the small oscillation with frequency  $\Omega_n = q_n \sqrt{v_n}$  about periodic trajectory  $r_n$ . Phase  $\varphi$  is related to the stability parameter of periodic trajectory, or Greene's residue  $R = \sin^2(\varphi/2)$ . In particular,  $R_\infty(r_g) = 0.2500888 \dots$  /23/. This is also an important characteristic of scale invariance, and it is related to  $A_\infty$  by

$$A_\infty(r_g) = \frac{5}{4\pi^2} \varphi_\infty^2(r_g) = 0.139 \quad (4.11)$$

in a reasonable agreement with numerical value (4.9) from the Fourier spectrum.

The above relations also permit to calculate the set of residues  $R_n$  (or  $\varphi_n$ ) for periodic trajectories  $r_n$  at a given  $K$  or that of  $K_n$  for a given  $R$ . From the former data in Ref: /27/ (see Eq. (3.21) there) the factor  $C = -\beta_0 \ln r_g \approx 1.11$  which is rather close to the above value. However, the gradient  $K'_\ell$ , as obtained from the same data in Ref. /23/, turns out to be quite different

$$K'_\ell = \frac{\sqrt{5} B_R}{C R_\infty} \approx 0.354 \quad (4.12)$$

where we have used  $C = 1.11$ , and where  $B_R \approx 0.0439$  is a constant in the standard scale invariance relation /23/:

$$R_n = R_\infty + B_R \cdot \delta_R^{1-n} \quad (4.13)$$

Here the convergence parameter

$$\delta_n = \frac{R_n - R_{n-1}}{R_{n+1} - R_n} \rightarrow \delta_R \approx -s_g \approx -1.618 \quad (4.14)$$

according to the resonant theory, while its numerical value is  $\delta_R \approx -1.635$  /23/. The residue dynamics in  $n$  is also depicted in the upper part of Fig. 4 (after Ref. /23/).

Assume now that the above relations hold not only for the "golden mean"  $r=r_g$  but also in some neighborhood (in  $K_c$  actually). Then, one immediate conclusion from Eq. (4.10), where we keep the same value for  $\varphi_\infty = \varphi_\infty(r_g)$ , would be a shift in  $R_\infty(r^{(m)})$  for those special  $r^{(m)} = (m, m, \dots) = (\sqrt{m^2+4}-m)/2$  which obviously retain an exact scale invariance /25/. The shift is due to a different limiting value of the detune

$$|\sqrt{5}q\tilde{v}|_\infty = \sqrt{\frac{5}{m^2+4}} \quad (4.15)$$

whence

$$R_\infty(r^{(m)}) \approx \left(\frac{5}{m^2+4}\right)^{2-\mu} \cdot R_\infty(r_g) \quad (4.16)$$

This is the case, indeed, at least, qualitatively! According to numerical data in Ref. /27/  $R_\infty(r^{(2)}) = 0.23 \pm 0.01$  ( $K_c(r^{(2)}) = 0.9574\dots$ ) while Eq. (4.16) gives  $R_\infty = 0.20$ . Instead, we may calculate  $\mu$  value to obtain:  $\mu = 1.64 \pm 0.18$ .

### 5. Renormalization Chaos

Representation of the renormgroup as a dynamical system is instructive, particularly, in that it suggests a more rich critical phenomena than just a fixed point, i.e. exact scale invariance. The opposite limiting case would be a chaotic dynamics that is a random variation of critical structure from one scale to the next. Such a possibility was discussed in Refs. /17,29/, and is implicitly present in Ref. /23,25/.

As we have seen in the previous Section the critical struc-

ture depends, particularly, on renormalization dynamics of detune  $(\sqrt{5}q\tilde{v})_n$ . The latter is determined, in turn, by arithmetical properties of the rotation number  $r$ . It is easy to verify that the dynamics of frequency ratio  $u_n = -v_n/v_{n-1} (>0)$  is described by the mapping

$$u_n = \frac{1}{u_{n-1}} \mod 1; \quad \left[ \frac{1}{u_{n-1}} \right] = m_n \quad (5.1)$$

with the initial  $u_0 = r = (m_1, m_2, \dots, m_n, \dots)$ . Then, for almost any  $r$  the sequence  $\{u_n\}$  is random since its KS-entropy  $h = \pi^2/6 \ln 2 > 0$  (see Ref. /12/). Apparently, the sequence  $\{m_n\}$  is also random as well as  $\{q_n\}$  ( $q_n = m_n q_{n-1} + q_{n-2}$ ), and  $\{q_n v_n\}$  too. The dynamics of  $q_n$  can also be described by the map (5.1) using the ratios  $w_n = q_{n-1}/q_n$ . Then, backwards in renormtime  $n$

$$w_{n-1} = \frac{1}{w_n} \mod 1; \quad \left[ \frac{1}{w_n} \right] = m_n \quad (5.2)$$

with the "final" condition  $w_1 = 1/m_1$  and rational  $w_n$  only. The "initial" condition for map (5.2) is irrational  $w_\infty$  with reversed sequence of the elements  $m_i$ . Since the set of such numbers has the full measure, the sequence  $w_n$  has the same statistical properties as those of  $u_n$ , and the average ratio of successive denominators is given by (see Ref. /12/):

$$\langle \ln w \rangle = -\frac{h}{2}; \quad S = \langle \frac{1}{w} \rangle = \langle \frac{q_n}{q_{n-1}} \rangle = e^{h/2} \approx 3.28 \quad (5.3)$$

An example of the critical structure for a random

$$r = r_{\text{RAND}} = (2, 1, 1, 1, 2, 1, 2, 1, 1, 1, 2, 1, 1, 1, 2, 1, \dots) = 0.37966453... \quad (5.4)$$

is also depicted in Fig. 4. The data have been obtained from the periodic trajectory with  $q_N = 10612$  ( $|r_N - r_{\text{RAND}}| \sim 10^{-8}$ ) at  $K = 0.9618704$ . The change in renormalization behavior is striking: a big Fourier amplitude variation is apparently irregular, and shows no obvious trend to decay. The same is true for  $R_n$  variation as well. Note that  $r_{\text{RAND}}$  is close to another "golden"  $r = 1 - r_g = (2, 1, 1, \dots) \approx 0.382$ . In Fig. 5 the depen-



dence of  $|qa|$  vs.  $|\sqrt{5}q\tilde{v}|$  is plotted to see if power law (4.6) still holds. It does, indeed, to the accuracy of a few per cent, as the least square fit shows. Moreover, the parameters  $\mu \approx 1.37$  and especially  $A_\infty(r_{RAND}) \approx 0.168$  are close to the "golden" ones (Sect. 4)\*). Note that the present  $\mu$  value is still closer to one for  $r^{(2)}$  (see above).

## 6. The Chaos Border and Statistical "Anomalies"

The chaos border in phase plane is always a critical curve. However, neither exact location of this curve nor its rotation number are known beforehand. Therefore, this problem turns out to be much more complicated than the previous one. On the other hand, it is much more important. A given critical KAM curve corresponds to very particular values of the system parameters,  $K$ , for instance, in standard map. This is always an exceptional case. On the contrary, the chaos border generally exists in a wide range of parameters, its position and rotation number varying, while the critical structure persists.

As an example we consider the so-called separatrix mapping /13/:

$$\bar{y} = y + \sin \theta; \quad \bar{\theta} = \theta - \lambda \cdot \ln |y| \quad (6.1)$$

with the only parameter  $\lambda$ . This model approximately describes, for example, the particle motion in a mirror magnetic trap near the loss cone /2/. Map (6.1) reduces locally in  $y \approx z$  to the standard map with  $K = -\lambda/z$ , and  $-\bar{y} = \lambda \cdot \ln |z| + \lambda(y-z)/z$ . Roughly, the chaos border corresponds to  $|K| = K_G \approx 1$ , i.e. to  $|z| = z_g \approx \lambda$ , so that chaotic component of motion comprises the layer  $|y| \leq \lambda$ . The border rotation number  $r_g \approx -\frac{\lambda}{2\pi} \cdot \ln \lambda$ .

First numerical data on the structure of chaos border have been obtained in Ref. /26/ following the technique of Ref. /30/. The method was based upon the concept of Poincaré recurrences and consisted in computation of the probability  $P(z)$  for a random trajectory to recur after  $\tilde{z}$  iterations back to the layer center  $y = 0$ . The resulting numerical data for va-

\*) The same is also true for  $C$  in Eq. (4.5) which is equal to 1.2 from  $a_n$ , and to 1.1 from  $R_n$ .

rious  $\lambda$  from  $\lambda = 1(+)$  through  $\lambda = 100$  (■) are shown in Fig. 6 (after Ref. /26/). Roughly, the dependence  $P(\tau)$  looks, at average, like a power law:

$$P(\tau) = \frac{B(\lambda)}{\tau^\rho} \quad (6.2)$$

For small  $\tau$  the exponent  $\rho = 1/2$ , and  $B = 1$  independent of  $\lambda$ . It is explained by a homogeneous diffusion inside the layer until its border is reached. This is just the recurrence behavior which was observed in Ref. /30/. At a larger  $\tau$  the dependence changes abruptly. The overall average  $\langle \rho \rangle = 1.45$  with a fairly big dispersion from  $\rho = 1.26$  ( $\lambda = 30$ ) through  $\rho = 1.64$  ( $\lambda = 1$ ). This latter behavior of recurrences is apparently related to the structure of the chaos border /26/. A power law dependence suggests some scale invariance of this structure. Apparently irregular oscillations in  $P(\tau)$ , clearly seen in Fig. 6, are also a very important peculiarity of the recurrence behavior. Moreover, they do not depend on the initial conditions in spite of motion instability. This suggests their relation to the chaos border structure too. A similar behavior was observed in a rather different (but also two-dimensional) mapping in Ref. /16/. The oscillation in  $P(\tau)$  has been interpreted in Ref. /17/ as an indication of the renormchaos for most values of parameter  $\lambda$ .

An attempt to analytically evaluate the critical exponent  $\rho$  was made in Refs. /26,24/. The main idea was in that the diffusion rate  $D \propto \rho^\alpha$  is rapidly approaching zero near the chaos border ( $\rho = r - r_b > 0$ ). For  $\alpha > 2$  the diffusion equation

$$\frac{\partial f}{\partial t} = \frac{\partial}{\partial \rho} \rho^\alpha \frac{\partial f}{\partial \rho} \quad (6.3)$$

has no eigenfunctions which are regular at  $\rho = 0$ . This leads particularly, to a nonexponential (power law) relaxation. For the critical exponent in Poincaré recurrences the following relation has been derived

$$\rho = 1 + \frac{1}{\alpha - 2} \quad (6.4)$$

The exact solution of the problem is possible by means of the Green function for Eq. (6.3) which has been found by Meiss /31/. It confirms Eq. (6.4).

A more hard task is evaluation of the diffusion rate critical exponent  $\alpha$ . Using the resonant theory, outlined in Sect. 4 above, the value  $\alpha = 5/2$  has been obtained in Ref. /24/. It gives  $\rho = 3$  in a plain contradiction with the numerical data. A possible explanation for this discrepancy is the following. The transit time  $\tau_n$  between neighboring scales of the critical structure needs not to be of the border of corresponding time scale  $t_n \sim q_n$  as was assumed in Ref. /24/. According to Refs. /21,32/ the transit time is determined by crossing some crucial invariant cantorus which replaces the corresponding critical KAM curve for a supercritical perturbation. Particularly, the following scaling has been obtained in Ref. /21/ for the transit time between neighboring integer (principal) resonances ( $J_n = 2\pi n$ ) in standard map

$$\tau \propto \varepsilon^{-\eta} \quad (6.5)$$

where  $\varepsilon = K - K_c$ , and  $\eta = 3.0117... \approx 3$ .

This result has been applied to the chaos border problem /17/ assuming  $\varepsilon \propto \rho$  near the border so that  $\varepsilon > 0$  at the chaotic side,  $\varepsilon < 0$  at regular side, and  $\varepsilon = 0$  on the border. It gives

$$\rho = 1 + \frac{2}{1+2\eta} \approx \frac{9}{7} \approx 1.29; \quad \alpha = \frac{5}{2} + \eta \approx \frac{11}{2} \quad (6.6)$$

which somewhat underestimates numerical value of  $\rho \approx 1.4$ .

Here we consider another approach to the problem. First, we derive Eq. (6.5). The crucial invariant cantorus, responsible for Eq. (6.5), is embedded into a chaotic layer whose width is determined by the biggest scale ( $q_c$ ) (principal resonance) of critical structure destroyed by a supercritical perturbation  $\varepsilon > 0$ . Then, from Eq. (4.5)  $q_c \sim \varepsilon^{-1}$ . The crossing time for this chaotic layer is of the same order. Since scale  $\rho_c \sim q_c^{-2}$  /24/, the transit time out of a large domain  $\rho_c \gg \rho$  through the chaotic layer is

$$\tau \sim q_c \frac{\rho_c}{\rho_c} \propto q_c^3 \sim \varepsilon^{-3} \quad (6.7)$$

in a fairly good agreement with Eq. (6.5).

Now we turn to the chaos border. Since, by assumption,  $\varepsilon_n \sim \rho_n \sim q_n^{-2}$  the period  $Q_n$  of the crucial cantorus on scale  $n$  is

$$Q_n \sim \varepsilon_n^{-1} \sim q_n^2 \gg q_n \quad (6.8)$$

Hence, this cantorus corresponds not to one of the principal resonances for the border rotation number  $r_\partial$  but to an intermediate resonance (see Fig. 3), or to a principal resonance of some intermediate rotation number  $r'_n$  ( $p_n/q_n < r'_n < p_{n-2}/q_{n-2}$ ). We assume in Eq. (6.8) that exponential dependence (4.5) holds qualitatively for such intermediate resonances as well. The latter is confirmed by our numerical data. Assuming, further, just one (or a few) crucial cantori on each scale and using Eq. (6.7) we arrive at the following estimate for the transit time

$$\tau_n \sim Q_n \left( \frac{Q_n}{q_n} \right)^2 \sim q_n^4 \sim \rho_n^{-2} \quad (6.9)$$

whence the diffusion rate and critical exponents are

$$D \sim \frac{\rho^2}{\tau} \sim \rho^4; \quad \alpha = 4; \quad \beta = \frac{3}{2} \quad (6.10)$$

The latter number seems to somewhat overestimate numerical value of  $\beta \approx 1.4$  although one should bear in mind uncertainties in the numerical value mentioned above. The remaining discrepancy, if any, may be related to the fact that there are actually many crucial chaotic layers on each scale. This important, and as yet unsolved, question is discussed in Ref. /21/.

The statistic of Poincaré's recurrences mainly serves just as a convenient way for studying statistical "anomalies" of the chaotic motion with a chaos border. Yet, it is also closely related to a more important statistical property, the correlation. Consider, for example, a correlating function

which is approximately constant at chaos border. Then, the correlation  $C(\tau) \sim \rho(\tau)$  as  $\tau \rightarrow \infty$ , and Eq. (6.9) gives (see Refs. /16,26/)

$$C(\tau) \sim \frac{1}{\tau^{p-1}} = \frac{1}{\sqrt{\tau}} \quad (6.11)$$

Note that the latter law (for  $p = 3/2$ ) is the same as for one-dimensional, homogeneous and unbounded diffusion. The spectrum of correlation, or the "power" spectrum of motion, as  $\omega \rightarrow 0$ , has the form

$$S(\omega) \propto \frac{1}{\omega^{2-p}} = \frac{1}{\sqrt{\omega}} \quad (6.12)$$

The law  $1/\omega$  is reached here for  $p \rightarrow 1$  only that is for an indefinitely slow correlation decay. However, for any  $p < 2$ , i.e. for critical correlation exponent  $(p-1) < 1$ , the spectrum is singular at  $\omega = 0$  while the integral "power" within the interval  $(0, \omega)$  vanishes with  $\omega$  if  $p > 1$ .

If a slowly decaying correlation determines, in turn, some other diffusion, the statistical "anomalies" become even more "grave". Indeed, the diffusion rate is proportional to the integral of correlation, which diverges if  $(p-1) < 1$ . The diffusion in standard map for special  $K \approx 2\pi n$  ( $n \neq 0$  integer) is an example. The usual diffusion equation is completely inapplicable in this case since the process to be described is essentially non-Markovian, and the formally defined diffusion rate grows indefinitely with time /15-17/:

$$D = \frac{\langle (\Delta y)^2 \rangle}{t} \propto t^{2-p} \quad (6.13)$$

It simply means that the second moment of distribution function (its width squared) grows faster than time:  $\langle (\Delta y)^2 \rangle \propto t^{3-p}$ . Numerical simulations with various models confirm this conclusion /15-17/. However, the problem of complete statistical description for such an "abnormally" fast diffusion still remains to be solved.

### Acknowledgements

I take this opportunity to express my sincere gratitude to D.L.Shepelyansky, in collaboration with whom many results presented above have been obtained, to A.A.Brudno, R.S.MacKay, J.Meiss, I.C.Percival and F.Vivaldi for stimulating discussions, and to L.P.Kadanoff for providing many of his published and unpublished papers on the critical phenomena in dynamics.

## References

- /1/ LICHTENBERG, A.J., and LIEBERMAN, A.M., Regular and Stochastic Motion, Berlin, Springer-Verlag, 1983.
- /2/ CHIRIKOV, B.V., Particle Motion in Magnetic Traps, Voprosy teorii plazmy (Topics in Plasma Theory), Ed. B.B.Kadomtsev, Moskva, Energoatomizdat, 1984, Vol. 13, 3.
- /3/ BORA, D., JOHN, P.I., SAXENA, Y.C., and VARMA, R.K., Proc. Internat. Conf. on Plasma Physics, Nagoya, April 1980, Vol. I, 171.
- /4/ BORA, D., JOHN, P.I., SAXENA, Y.C., and VARMA, R.K., Plasma Phys., 22 (1980) 653.
- /5/ ALEKSEEV, V.M., and YAKOBSON, M.V., Phys. Reports, 75 (1981) 287.
- /6/ BRUDNO, A.A., Trudy Mosk. mat. obshchestva (Proc. Moscow Math. Soc.), 44 (1982) 124.
- /7/ FORD, J., Phys. Today, 36, No. 4 (1983) 40.
- /8/ CHIRIKOV, B.V., Proc. Internat. Seminar, Group Theoretical Methods in Physics, Zvenigorod, November 1982, Moskva, Nauka, 1983, Vol. II, 389.
- /9/ CASATI, G., CHIRIKOV, B.V., and FORD, J., Phys. Lett. A, 77 (1980) 91.
- /10/ BORN, M., Phys. Blätter, 11 (1955) 49.
- /11/ RECHESTER, A.B., ROSENBLUTH, M.N., Phys. Rev. Lett., 40, (1978) 38.
- /12/ KORNFELD, I.P., SINAI, YA.G., FOMIN, S.V., Ergodic Theory, Moskva, Nauka, 1980.
- /13/ CHIRIKOV, B.V., Phys. Reports, 52 (1979) 263.
- /14/ RECHESTER, A.B., and WHITE, R.B., Phys. Rev. Lett., 44 (1980) 1586.
- /15/ KARNEY, C.F.F., RECHESTER, A.B., and WHITE, R.B., Physica D, 4 (1982) 425.
- /16/ KARNEY, C.F.F., Physica D, 8 (1983) 360.

- /17/ CHIRIKOV, B.V., and SHEPELYANSKY, D.L., Correlation Properties of Dynamical Chaos in Hamiltonian Systems, *Physica D*, 13 (1984).
- /18/ VIVALDI, F., CASATI, G., and GUARNERI, I., *Phys. Rev. Lett.*, 51 (1983) 727.
- /19/ CHIRIKOV, B.V., IZRAILEV, F.M., and SHEPELYANSKY, D.L., *Soviet Scientific Reviews C*, 2 (1981) 209.
- /20/ OTT, E., et al., *Phys. Fluids*, 21 (1978) 2263; 22 (1979) 2247; 23 (1980) 1031; 25 (1982) 359.
- /21/ MACKAY, R.S., MEISS, J.D., and PERCIVAL, I.C., Transport in Hamiltonian Systems, *Physica D*, 13 (1984) 55.
- /22/ GREENE, J.M., *J. Math. Phys. (N.Y.)*, 9 (1968) 760; 20 (1979) 1183.
- /23/ MACKAY, R.S., Thesis, Princeton University, 1982; *Physica D*, 7 (1983) 283.
- /24/ CHIRIKOV, B.V., *Lecture Notes in Physics*, 179 (1983) 29.
- /25/ ESCANDE, D.F., *Physica Scripta*, T2/1 (1982) 126.
- /26/ CHIRIKOV, B.V., SHEPELYANSKY, D.L., *Proc. 9th Internat. Conf., Nonlinear Oscillations, Kiev, September 1981, Kiev, Naukova dumka, 1984, Vol. II, p. 421.* English translation is available as PPPL-TRANS-133, Plasma Physics Lab, Princeton University, 1983.
- /27/ SHENKER, S.J., and KADANOFF, L.P., *J. Stat. Phys.*, 27 (1982) 631.
- /28/ SCHMIDT, G., and BIALEK, J., *Physica D*, 5 (1982) 397.
- /29/ OSTLUND, S., RAND, D., SETHNA, J., and SIGGIA, E., *Physica D*, 8 (1983) 303.
- /30/ CHANNON, S.R., and LEBOWITZ, J.L., *Ann. N.Y. Acad. Sci.*, 357 (1980) 108.
- /31/ MEISS, J.D., private communication, 1983.
- /32/ BENSIMON, D., and KADANOFF, L.P., *Physica D*, 13 (1984) 82.



### Figure captions

- Fig. 1. Chaos in axisymmetric mirror trap: (1) adiabatic loss cone; (2) chaotic motion (leakage of particles); (3) regular motion (particle confinement); (4) chaos border (boundary of confinement).
- Fig. 2. Nonexponential electron relaxation in a mirror magnetic trap in semilog (circles) and log-log (dots) scales: (1), (2) the exponentials with  $\tau \approx 0.35$  and  $0.61$  msec; (3) the power law with exponent  $\rho \approx 2.2$ ; I the electron current out of the trap in arbitrary units.
- Fig. 3. A sketch of principal resonances of periods  $Q_n$  near critical curve  $\rho = r - r_c = 0$ . Two crucial chaotic layers with cantori of periods  $Q_{n+2}$  and  $Q_{n+3}$  are also shown (Sect. 6).
- Fig. 4. Critical renormalization dynamics in  $n$ , the serial number of scales (renormtime), for  $r = r_g$  (fixed point, or exact scale invariance, dots), and for a random  $r$  (5.4) (renormchaos, or statistical scale invariance, circles). Solid lines indicate one side of critical curves ( $\rho > 0$ ) while dashed lines do so for the other ( $\rho < 0$ ), cf. Fig. 3.
- Fig. 5. Reduced amplitudes  $qa$  vs. detune  $\sqrt{5}q\tilde{v}$  for a random  $r$  (5.4) in log-log scale. Straight line is the least square fit:  $|qa| \cdot |\sqrt{5}q\tilde{v}|^{1.37} = 0.168$ . The circle corresponds to  $r = r_g$  while arrow points  $|\sqrt{5}q\tilde{v}|_\infty$  for  $r = r^{(2)}$  (4.15).
- Fig. 6. Statistic of Poincaré recurrences in separatrix map (6.1) for  $\lambda = 1.100$ ;  $10^7$  iterations (after Ref. /26/). Upper line is Eq. (6.2) with  $\rho = 1/2$  and  $B = 1$ ; lower line shows the fit for  $\lambda = 3(\cdot)$ :  $\rho = 1.37$ ;  $B = 4.0$ .

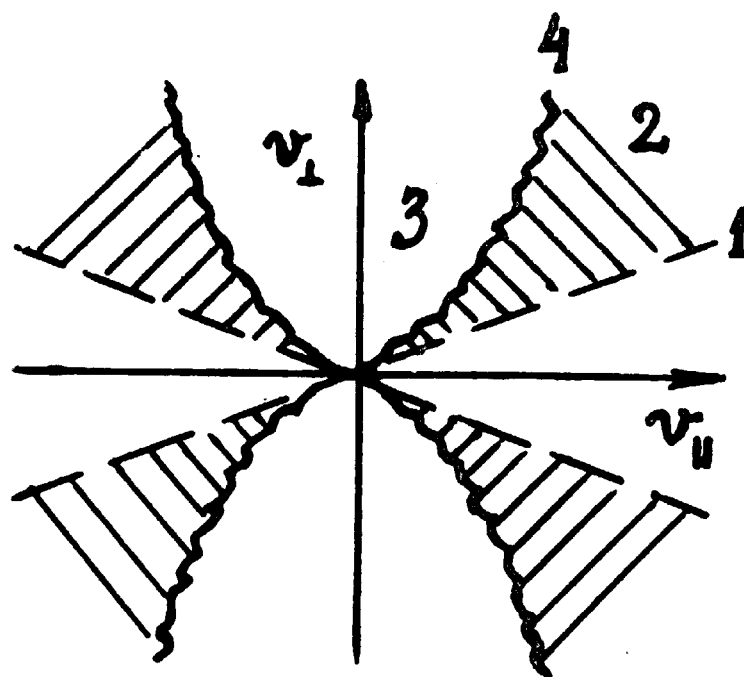


Fig. 1

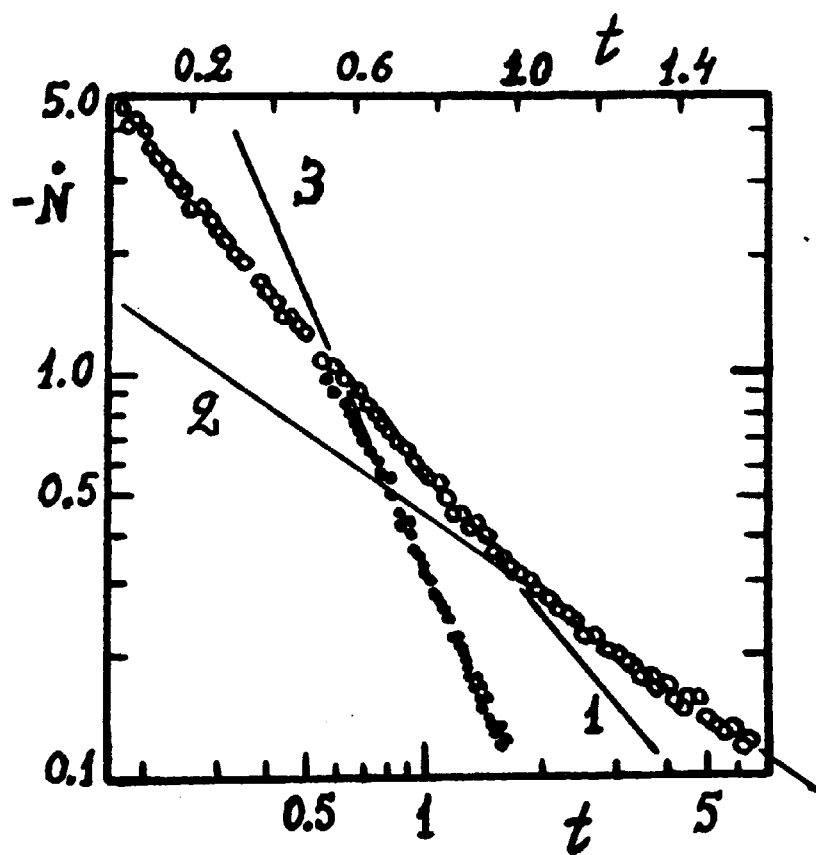


Fig. 2

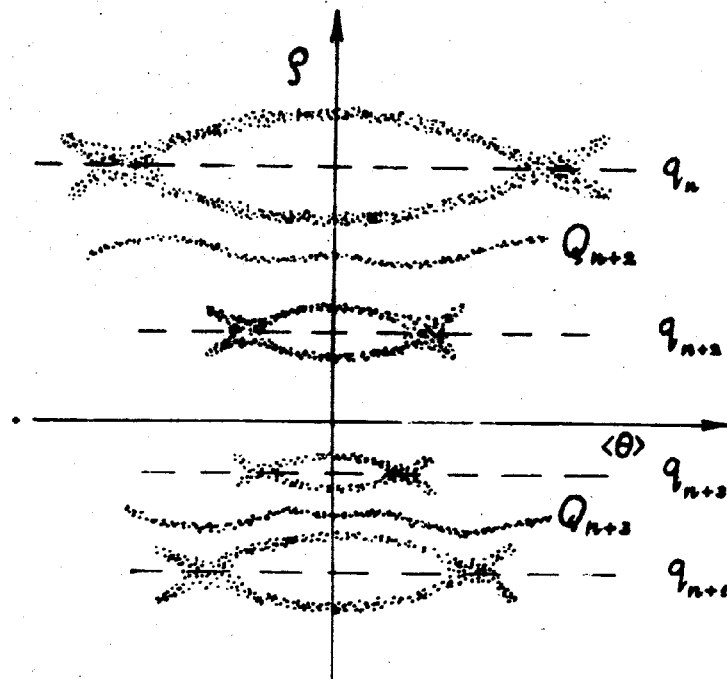


Fig. 3

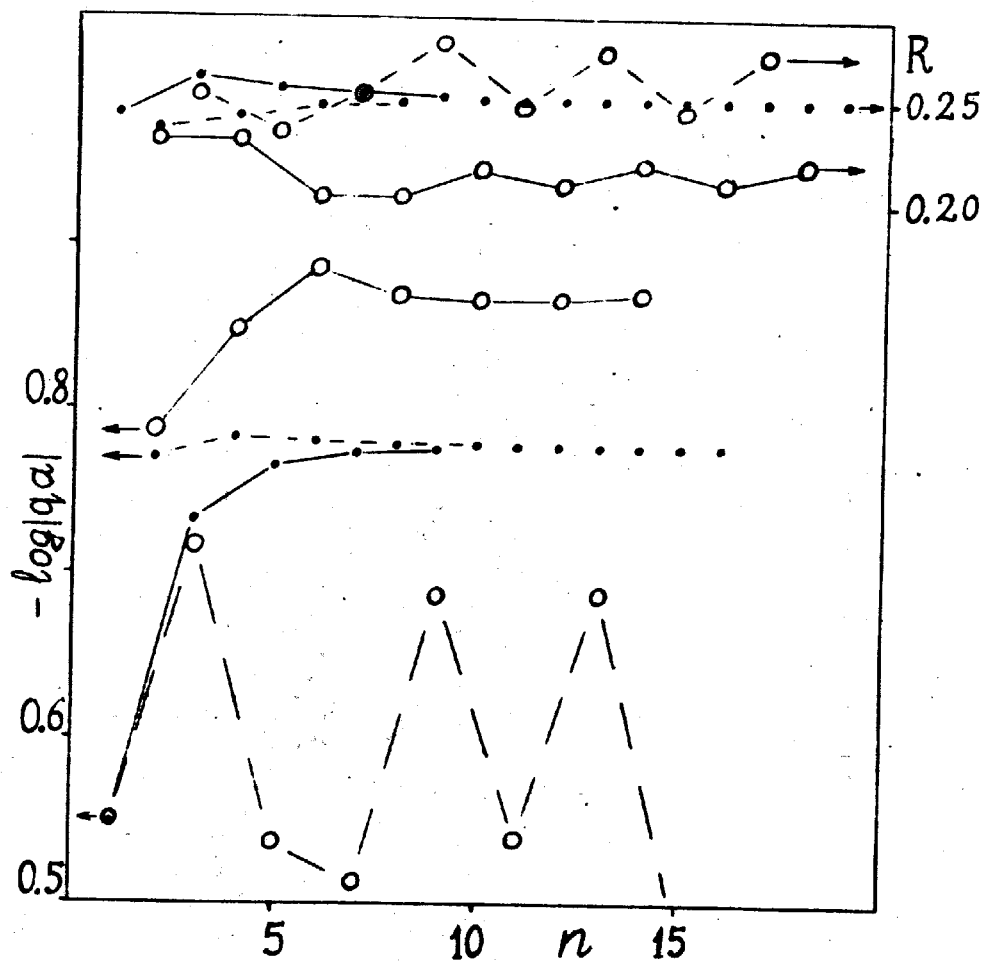


Fig. 4

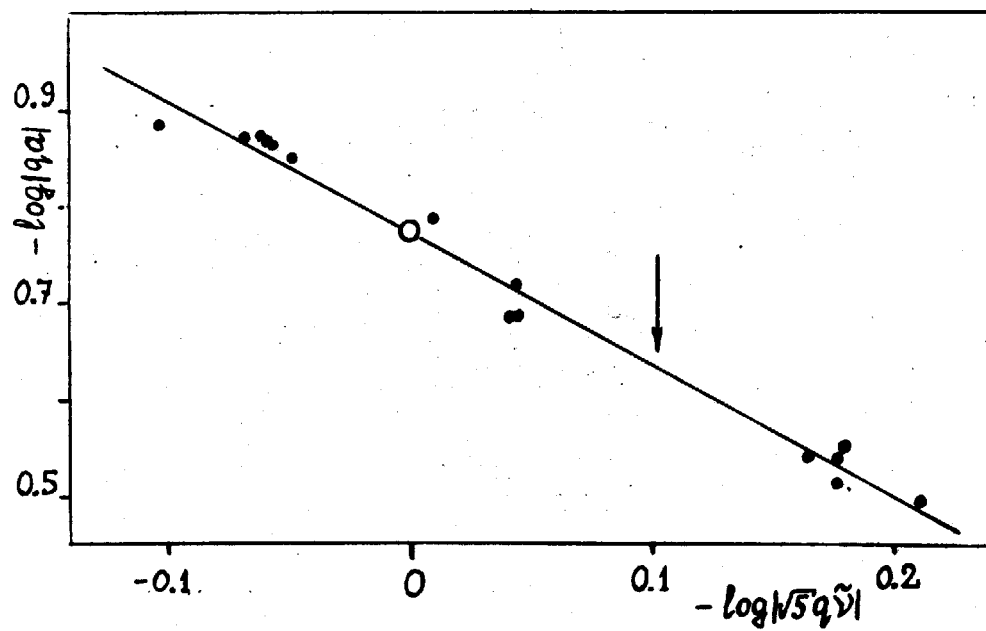


Fig. 5

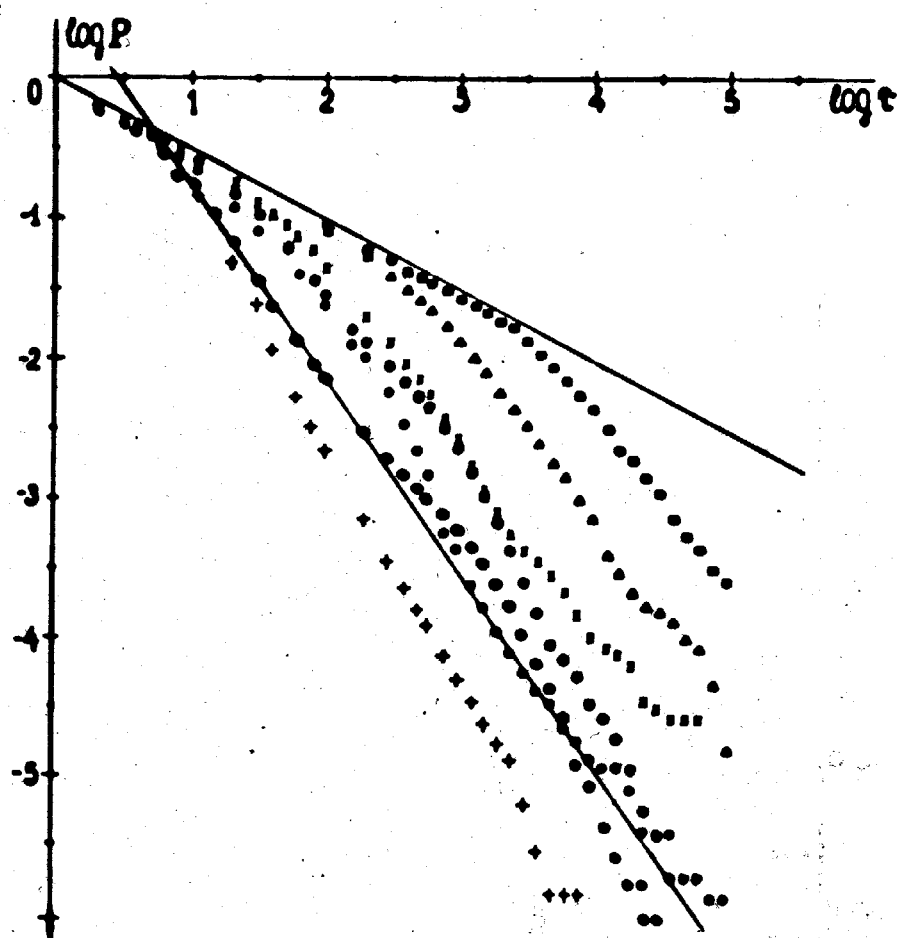


Fig. 6

Б.В.Чириков

ДИНАМИЧЕСКАЯ СТОХАСТИЧНОСТЬ

Препринт  
№ 84-147

Работа поступила - 2 ноября 1984 г.

---

Ответственный за выпуск - С.Г.Попов

Подписано к печати 16.XI-1984 г. МН 06217

Формат бумаги 60х90 1/16 Усл.2,0 печ.л., 1,6 учетно-изд.л.

Тираж 290 экз. Бесплатно. Заказ № 147.

---

Ротапринт ИЯФ СО АН СССР, г.Новосибирск, 90